Journal of Sound and Vibration (2001) **243**(4), 747–761
doi:10.1006/jsvi.2000.3420, available online at http://www.idealibrary.com on IDEAL®

ATTENUATION OF STRESS WAVE PROPAGATION IN PERIODICALLY LAYERED ELASTIC MEDIA

C. Han and C. T. Sun

*School of Aeronautics and Astronautics, Purdue University, W. Lafayette, IN*47907-1282

(*Received* 1 *October* 1999, *and in final form* 24 *October* 2000)

An exact viscoelastic analogous relation between a periodically layered elastic medium and a homogeneous viscoelastic medium was introduced, based upon which a short-time relaxation function was developed. Both the wave front decay and the spatial attenuation of stress waves in a periodically layered medium were studied. It was shown that the spatial attenuation of long waves propagating in a periodically layered elastic medium describes the attenuation of the wave trailing the wave front, while the spatial attenuation of a short wave characterizes the wave front decay. The effects of thickness ratio of the two constituent layers, their mechanical properties, and the cell thickness on the attenuation of stress wave propagation were examined. The results showed that the use of the short-time analogous relaxation function is valid for the attenuation analysis of stress waves propagating in a periodically layered elastic medium.

1. INTRODUCTION

The behavior of wave propagation in layered media has been studied for decades. In his study, Barker [1] first reported that there was an analogy between layered elastic media and homogeneous viscoelastic media in terms of stress wave propagation, but he did not explain the analogy in a rigorous manner. Starting from a periodically layered viscoelastic medium in which a periodically layered elastic medium was a special case, Ting and Mukunoki [2, 3] theoretically proved Barker's finding. They showed that the analogy could be established in different ways. Ting and Mukunoki [2, 3] did not illustrate the wave attenuation effect for wave propagation in layered media because of the viscoelastic analogies. Christensen [4, 5] studied the same problem by using the perturbation method and dielectric theory, and derived an approximate spatial attenuation factor, which indicated the effect of viscoelastic analogy for only randomly layered media. Another work close to this paper was done by Karal and Keller [6], who found a frequency-independent attenuation factor for a randomly layered medium slightly different from a homogeneous elastic medium. Regardless of the correctness of the result presented in reference [6], its application is certainly very limited because layered media are often highly heterogeneous in practice.

In this paper, we intended to define and demonstrate the attenuation effect implied by the viscoelastic analogy of a periodically layered elastic medium. Layered media constituted by two distinct elastic materials were studied. Wave front decay and spatial attenuation were studied and differentiated from each other. The spatial attenuation for time harmonic stress waves was introduced to explain the apparent attenuation phenomenon of the wave trailing

0022-460X/01/240747 + 15 $35.00/0

the wave front in the periodically layered elastic medium. The relationship between the attenuation and the typical cell thickness and layer thickness ratio was examined. Different material combinations of layers were also investigated.

2. VISCOELASTIC ANALOGY

2.1. ANALOGY IN SOLUTION FORM

Consider a periodically layered elastic medium as shown in Figure 1. A typical cell of thickness h consists of two constituent layers with distinct properties. The odd-numbered layers (layers 1, 3, 5, …) are of material 1 with a layer thickness h_1, density ρ_1, and the Lamé constants λ_1 and μ_1; and the even-numbered layers (layers 2, 4, 6, …) are of material 2 with layer thickness h_2, density ρ_2, and Lamé constants λ_2 and μ_2. For plane waves propagating normal to the layers, a stress analogy between such a layered elastic medium and a homogeneous viscoelastic medium can be established by a relaxation function $G(t)$ expressed in the Laplace transform domain as $\bar{G}(s)$ [2]:

$$\cosh\left(h\sqrt{\frac{\rho}{\bar{G}(s)}\,s}\right) = \theta\cosh(\alpha s) - (\theta - 1)\cosh(\beta s), \tag{1}$$

where s is the Laplace transform variable, and

$$\theta = \left(1 + \sqrt{\frac{\rho_1(\lambda_1 + 2\mu_1)}{\rho_2(\lambda_2 + 2\mu_2)}}\right)^2 \Bigg/ \left(4\sqrt{\frac{\rho_1(\lambda_1 + 2\mu_1)}{\rho_2(\lambda_1 + 2\mu_2)}}\right), \qquad \rho = \frac{h_1}{h}\rho_1 + \frac{h_2}{h}\rho_2, \tag{2, 3}$$

$$\alpha = \sqrt{\frac{\rho_1}{\lambda_1 + 2\mu_1}}\,h_1 + \sqrt{\frac{\rho_2}{\lambda_2 + 2\mu_2}}\,h_2, \qquad \beta = \sqrt{\frac{\rho_1}{\lambda_1 + 2\mu_1}}\,h_1 - \sqrt{\frac{\rho_2}{\lambda_2 + 2\mu_2}}\,h_2 \tag{4, 5}$$

It is obvious that the analogous relaxation function (1) is dependent on both material and geometry.

The stress solution in a homogeneous viscoelastic medium is given by Ting and Mukunoki [2]

$$\bar{\Phi}(s) = \bar{p}(s)\mathrm{e}^{\sqrt{(\rho s)/(\bar{G}(s))}\,x}, \tag{6}$$

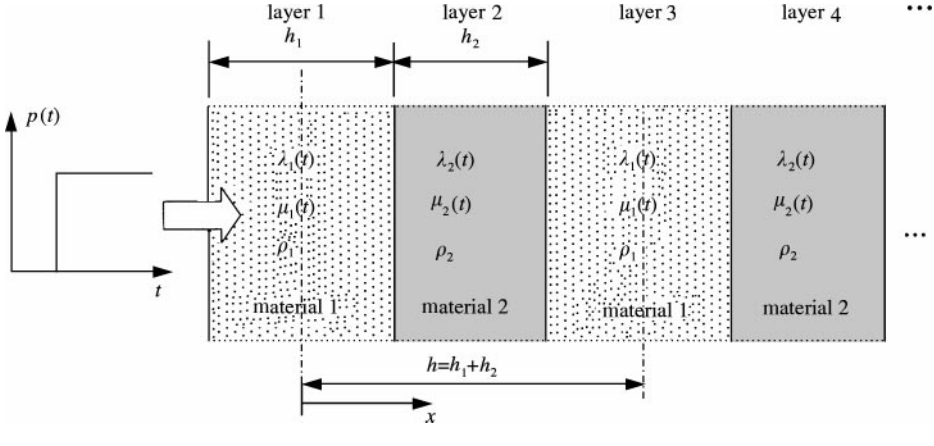

Figure 1. A periodically layered medium.

where $\bar{\Phi}(s)$ is the Laplace transform of the plane longitudinal stress in the homogeneous viscoelastic medium; $\bar{p}(s)$ is the Laplace transform of the initial stress condition at $(x = 0)$. The analogy given by equation (1) is that the stress response of a homogeneous viscoelastic medium with a relaxation function (1) is the same as the stress response of a periodically layered medium at the correspondent positions, which are located at the mid-planes of the odd-numbered layers (see Figure 1) given that the initial conditions are identical [2, 3]. To make this analogy valid, x in equation (6) should be taken as $n \times h$ $(n = 0, 1, 2, \ldots)$, so that the simple form (6) can be used to find a stress response in a periodically layered elastic medium. Solutions for arbitrary positions are also available in references [2, 3]. Since our interest was the attenuation effect of wave propagation in a layered medium, we did not list other solutions here for brevity.

2.2. ANALOGY IN WAVE FRONT DECAY

A wave front in a periodically layered elastic medium decays due to reflection at the interfaces. For a wave front having passed through a typical cell consisting of two constituent layers, it can be shown by analyzing the reflection and transmission of a wave that its wave front intensity decays as

$$\phi = \theta^{-1}\phi_0, \tag{7}$$

where ϕ is the intensity of the output wave front after the passage of a typical cell, θ is defined by equation (2), and ϕ_0 is the intensity of the incident wave front [2, 7]. If a wave front passes through n typical cells, its intensity ϕ is

$$\phi = \theta^{-n}\phi_0. \tag{8}$$

The wave front in a homogeneous viscoelastic medium also decays but due to viscous dissipation. Given a homogeneous viscoelastic medium represented by a relaxation function $G(t)$, it is shown in references [2, 8] that the wave front intensity Φ decays as

$$\Phi = \Phi_0 \mathrm{e}^{-\gamma x}, \tag{9}$$

where γ is called the wave front decay factor and can be given as

$$\gamma = -\frac{\dot{G}(0)}{2c_0 G(0)} \tag{10}$$

and c_0 is the speed of sound in the viscoelastic medium, $\dot{G}(0)$ is the derivative of $G(t)$ with respect to time t at $t = 0$, and Φ_0 is the intensity of the incident wave front.

Comparing equations (7) or (8) and equation (9), the two wave front decays can be made identical after the wave fronts propagate through the same distance in a periodically layered elastic medium and in a homogeneous viscoelastic medium, respectively, if the following holds:

$$\gamma = \frac{\ln \theta}{h}. \tag{11}$$

Note that the analogy relation (1) was not used in the derivation of decay of the wave front. Also note that the decay of the wave front is not influenced by the volume fraction factor (i.e., geometry parameters such as h_1 and h_2).

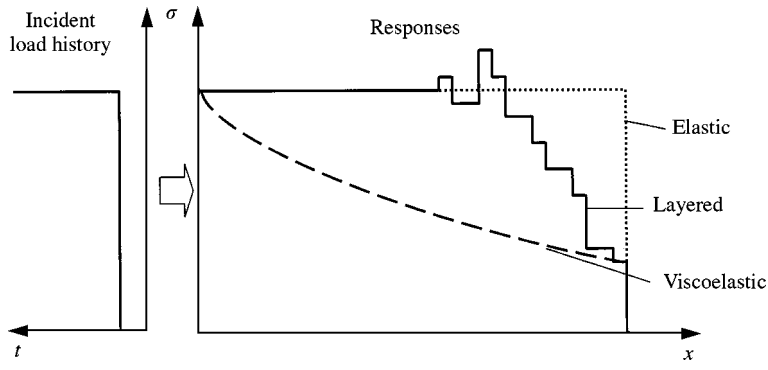

Figure 2. Schematic of a step stress wave propagating in three kinds of media.

Figure 2 is an illustration of a step stress wave propagating in a homogeneous Maxwell viscoelastic medium, a periodically layered elastic medium, and a homogeneous elastic medium respectively. The wave motion in the periodically layered elastic medium, except for the wave front, is different from that in a homogeneous viscoelastic medium, so it is different from that in a homogeneous elastic medium. This suggests that the analogy given by equation (1) describes the wave behavior in a periodically layered elastic medium different from that in a homogeneous viscoelastic medium. In the following section the unique attenuation characteristics of periodically layered elastic media will be found.

3. SPATIAL ATTENUATION

The difference of wave propagation in a periodically layered elastic medium and a homogeneous viscoelastic medium was the wave response trailing the wave front. Such a difference could be seen in the spatial wave profiles in Figure 2. Thus, the analogy of equation (1) needs further interpretations. As an attempt to differentiate the periodically layered medium and its analogous viscoelastic medium, consider plane time harmonic waves in a homogeneous viscoelastic medium, for which the displacement can be expressed in the form [8]

$$u(x, t) = \hat{u}\mathrm{e}^{-\eta x}\mathrm{e}^{\mathrm{i}\eta^*(x+\omega t/\eta^*)}, \tag{12}$$

where $\hat{u}$ is the constant amplitude, η is the attenuation factor, η^* is wave number (real), ω is frequency, and $\mathrm{i} = \sqrt{-1}$. It can be shown that the spatial attenuation [8, 9] factor is given by

$$\eta = \omega\rho^{1/2}G^{IV}/|G^*|, \tag{13}$$

where $G^* = G_1 + \mathrm{i}G_2$ is the complex modulus and G^{IV} is given by

$$G^{IV} = \mathrm{Im}(\sqrt{G^*}). \tag{14}$$

To complete the analogy, we need to find G^* and G^{IV} for a layered medium.

The relaxation function in the time domain, $G(t)$, can be obtained from equation (1) numerically. Given $G(t)$, the Kronig–Kramers integral relations [10] can be applied to solve

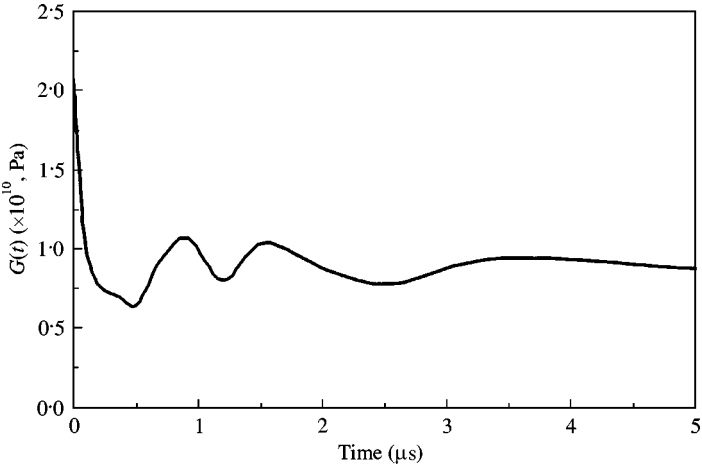

Figure 3. Illustration of the relaxation function of a layered medium ($\rho_1 = 7{\cdot}89 \times 10^3$ kg/m^3, $\lambda_1 = 110 \times 10^9$ Pa, $\mu_1 = 79 \times 10^9$ Pa, $h_1 = 0{\cdot}25 \times 10^{-3}$ m; $\rho_2 = 1{\cdot}15 \times 10^3$ kg/m^3, $\lambda_2 = 8{\cdot}9 \times 10^9$ Pa, $\mu_2 = 0$, $h_2 = 0.784 \times 10^{-3}$ m).

for G_1 and G_2. We have

$$G_1 = G(\infty) + \omega \int_0^\infty [G(t) - G(\infty)] \sin(\omega t)\, \mathrm{d}t, \tag{15}$$

$$G_2 = \omega \int_0^\infty [G(t) - G(\infty)] \cos(\omega t)\, \mathrm{d}t. \tag{16}$$

From equations (1) and (13)–(16), the spatial attenuation factor η can be obtained numerically if not analytically.

It seems that based upon the analytical relaxation function (1), we should readily find the attenuation factor. However, the computation yielded a vanishing attenuation factor. This is because the analogous relaxation function $G(t)$ defined by equation (1) does not monotonically decrease with time as a conventional relaxation function in viscoelasticity does [2, 3]. Figure 3 depicts a typical relaxation function of a layered elastic medium, which was obtained numerically by using the method of Legendre polynomials discussed in reference [11]. Although zero attenuation of a layered elastic medium sounds physically correct (which means there is no energy dissipation overall), it does not help us to explain the apparent attenuation near the wave front in a layered elastic medium.

From Figure 2, we note that a layered elastic medium behaves asymptotically as a homogeneous elastic medium for the wave at a distance behind the wave front. The differences in wave propagation occur at the wave front and its immediate waves. This observation leads to the notion that the viscoelastic analogy or attenuation effect of a layered elastic medium may be valid only for short-time responses.

The following is to derive a short-time analogous relaxation function for a periodically layered medium from the exact relaxation function (1).

3.1. SHORT-TIME ANALOGOUS RELAXATION FUNCTION

Recall the relation between the time domain variable t and the transform domain variable s in Laplace transform. Small t corresponds to large s, and *vice versa*. Considering

a large value of s and using the approximate expression

$$\cosh(s) = \tfrac{1}{2}\,\mathrm{e}^{s} + \cdots, \tag{17}$$

we obtain from edquation (1)

$$\mathrm{e}^{h\sqrt{\rho s}/\bar{G}(s)} = \theta \mathrm{e}^{\alpha s} - (\theta - 1)\mathrm{e}^{\beta s}. \tag{18}$$

From equations (4) and (5), we have $\alpha \geqslant \beta$. The equality case, $\alpha = \beta$, indicates that the layered medium degenerates into a homogeneous medium. Only the inequality case, $\alpha > \beta$, is considered.

Since s is very large and $\alpha - \beta > 0$, we simplified equation (18) and obtained the transformed relaxation function as

$$\bar{G}(s) = \frac{h^2 \rho s}{(\ln \theta + \alpha s)^2}. \tag{19}$$

The inverse transform of $\bar{G}(s)$ is easily obtained as

$$G(t) = \xi\left(1 - \frac{t}{\tau}\right)\mathrm{e}^{-t/\tau} \tag{20}$$

where

$$\tau = \alpha/\ln\theta, \qquad \xi = h^2\rho/\alpha^2. \tag{21}$$

Equation (20) represents an analogous relaxation function asymptotically approaching the exact one when t is small. Since we were only interested in the short-time response, we restricted the validity of $G(t)$ given by equation (20) only to $t \leqslant t_0$, where t_0 is solved from

$$\xi\left(1 - \frac{t_0}{\tau}\right)\mathrm{e}^{-t_0/\tau} = G_\infty. \tag{22}$$

G_∞ in equation (22) is the equivalent relaxation modulus and can be given as

$$G_\infty = G(\infty) = \frac{h(\lambda_1 + 2\mu_1)(\lambda_2 + 2\mu_2)}{h_1(\lambda_1 + 2\mu_1) + h_2(\lambda_2 + 2\mu_2)}. \tag{23}$$

Figure 4 shows the comparisons of the short-time relaxation function (labelled as "short-time") and the exact relaxation function (labelled as "exact") numerically obtained for (a) a layered medium consisting of steel/PMMA with a typical cell thickness of 1·034 mm and thickness ratio $h_1/h = 0{\cdot}24$ and (b) a layered medium composed of ceramic/aluminum with a typical cell thickness of 3 mm with thickness ratio $h_1/h = 0{\cdot}2$. The material properties are listed in Table 1. The symbols in Figure 4 are the values numerically calculated. It is evident that the derived short-time relaxation function agrees with the exact one very well.

Another comparison was the wave propagation in a layered medium by using the exact relaxation function (1) and by the short-time relaxation function (20). Figure 5 shows the two stress responses at the mid-plane of the 11th layer (layer 11, material 1) of the steel/PMMA medium subjected to a unit step stress loading. For case (a), $h = 1{\cdot}034$ mm, $h_1 = 0{\cdot}025$ mm; and for case (b) $h = 1{\cdot}034$ mm, $h_1 = 0{\cdot}25$ mm. The curves labelled as "exact" were obtained by using the exact relaxation function, while the ones labelled as "short-time" were computed by the short-time relaxation function. It is evident that the short-time relaxation function is able to characterize the behavior of a layered medium near the wave front.

In the sequel, we used the short-time relaxation function to study the attenuation of the wave trailing the wave front.

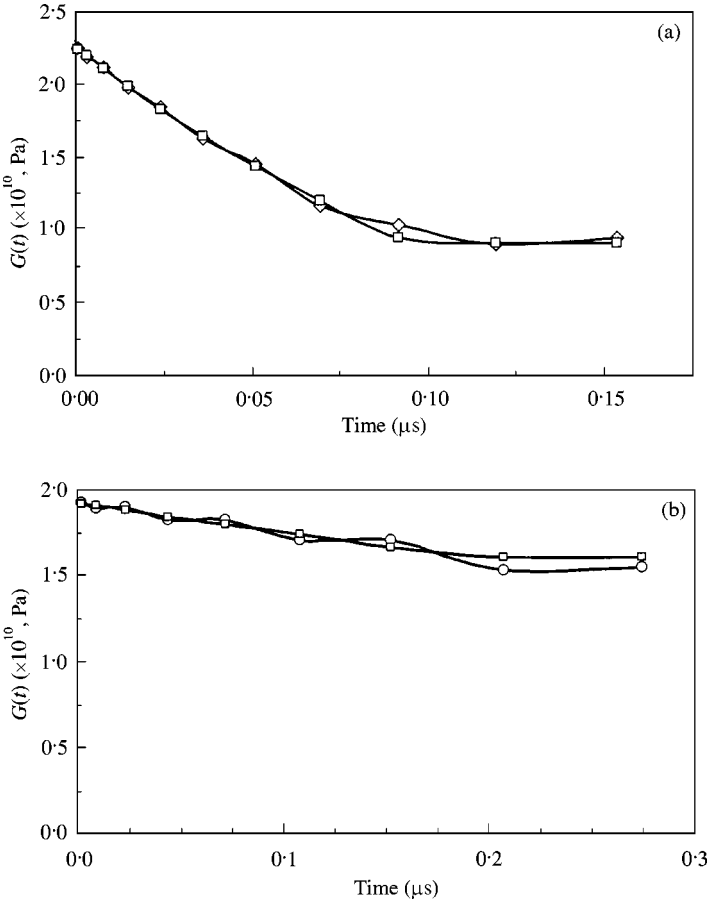

Figure 4. The exact relaxation function and the short-time relaxation function (—◇— exact; —□—, short time). (a) Steel/PMMA; (b) ceramic/aluminum.

TABLE 1

Material properties

Material No.	Material	Density (kg/m^3)	μ (GPa)	λ (GPa)	Impedance ratio (no. 1/ no. 2)
1	Steel	7·89	79	110	14
2	PMMA	1·15	0	8·9	
1	Ceramic	3·98	136	136	460
2	Rubber	1	0·0007	0·006	
1	Ceramic	3·98	107	128	2·5
2	Al	2·7	21	40	

Substituting equation (20) into equations (15) and (16) and neglecting the contribution to the integral after time t_0, one can find the complex modulus. After lengthy algebraic manipulations, we obtain

$$G_1(\omega) = G_\infty \cos \omega t_0 + \omega\xi(C_1 - C_3/\tau), \qquad G_2(\omega) = \omega\xi(C_2 - C_4/\tau) - G_\infty \sin \omega t_0, \quad (24, 25)$$

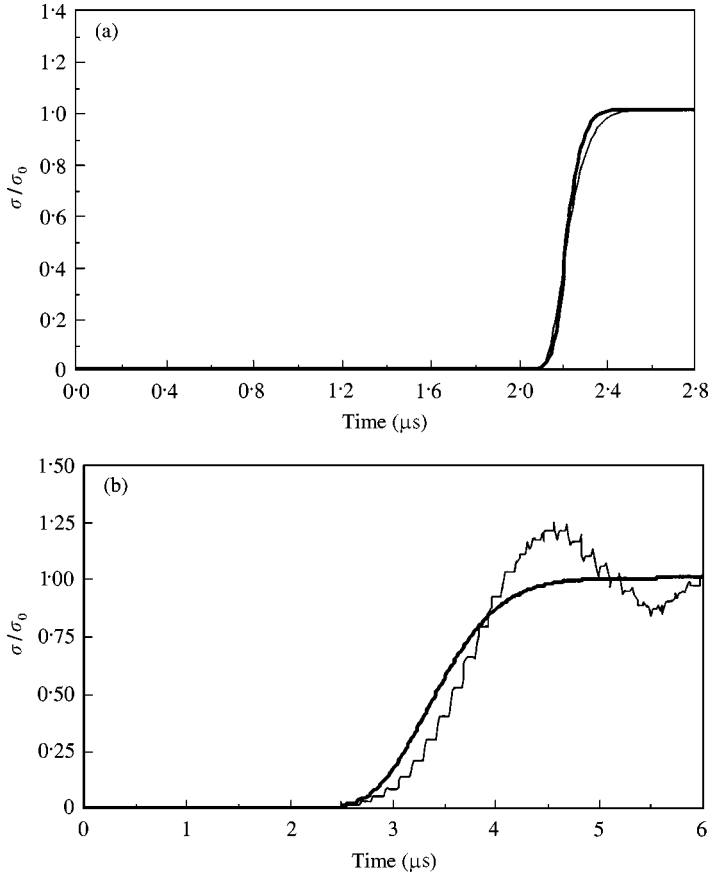

Figure 5. A step-stress wave propagating in a layered medium (——, exact; ▬, short time). (a) $h = 1{\cdot}034$ mm, $h_1 = 0{\cdot}025$ mm; (b) $h = 1{\cdot}034$ mm, $h_1 = 0{\cdot}25$ mm.

where

$$C_1 = \frac{1}{1/\tau^2 + \omega^2}\left[\omega - \left(\frac{\sin \omega t_0}{\tau} + \omega \cos \omega t_0\right)e^{-t_0/\tau}\right], \tag{26}$$

$$C_2 = \frac{1}{1/\tau^2 + \omega^2}\left[\frac{1}{\tau} - \left(\frac{\cos \omega t_0}{\tau} - \omega \sin \omega t_0\right)e^{-t_0/\tau}\right], \tag{27}$$

$$C_3 = \frac{-t_0 e^{-t_0/\tau}}{1/\tau^2 + \omega^2}\left(\frac{\sin \omega t_0}{\tau} + \omega \cos \omega t_0\right) - \frac{(1/\tau^2 - \omega^2)e^{-t_0/\tau} \sin \omega t_0}{(1/\tau^2 + \omega^2)^2} - \frac{2\omega(e^{-t_0/\tau} \cos \omega t_0 - 1)}{\tau(1/\tau^2 + \omega^2)^2}, \tag{28}$$

$$C_4 = \frac{t_0 e^{-t_0/\tau}}{1/\tau^2 + \omega^2}\left(-\frac{\cos \omega t_0}{\tau} + \omega \sin \omega t_0\right) - \frac{(1/\tau^2 - \omega^2)(e^{-t_0/\tau} \cos \omega t_0 - 1)}{(1/\tau^2 + \omega^2)^2} + \frac{2\omega e^{-t_0/\tau} \sin \omega t_0}{\tau(1/\tau^2 + \omega^2)^2}. \tag{29}$$

Consider two extreme cases, namely, long wave (small ω) and short wave (large ω). If $\omega \to 0$, the following approximations can be derived from equations (26)–(29):

$$C_1 \approx 0, \qquad C_2 \approx \tau(1 - e^{-t_0/\tau}), \qquad C_3 \approx 0, \qquad C_4 \approx \tau^2\left[1 - \left(1 + \frac{t_0}{\tau}\right)e^{-t_0/\tau}\right]. \tag{30}$$

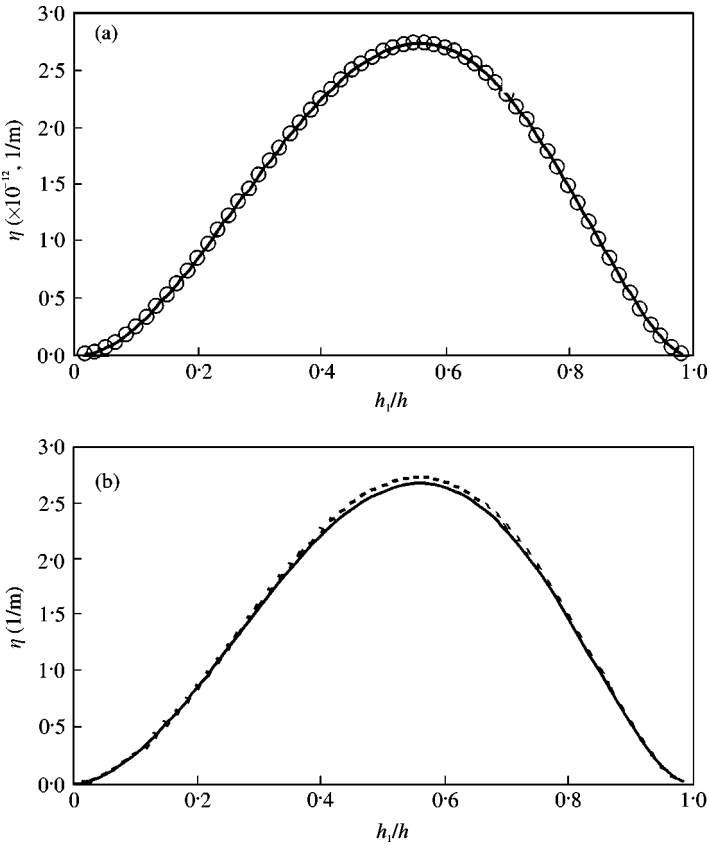

Figure 6. Spatial attenuation factors obtained from the short-time relaxation function with and without the long-wave assumption. (a) $\omega = 1$ Hz (○, short time; ——, long wave); (b) $\omega = 1$ MHz (——, short time; - - - -, long wave).

Substituting equation (30) into equations (24) and (25), and further simplifying, we have

$$G_1(\omega) \approx G_\infty, \qquad G_2(\omega) \approx \omega t_0(\xi e^{-(t_0/\tau)} - G_\infty). \tag{31, 32}$$

Using equations (31) and (32) and noting $G_1(\omega) \gg G_2(\omega)$ for small ω, we obtained, from equation (13), the spatial attenuation factor for long waves in a layered medium as

$$\eta = \frac{\omega^2 \rho^{1/2} t_0^2}{2(\tau - t_0) G_\infty^{1/2}}. \tag{33}$$

Equation (33) is compared with the spatial attenuation factor computed based upon the short-time relaxation function without the long wave assumption for frequencies 1 Hz and 1 MHz. Figure 6 shows that the two attenuation factors corresponding to these two frequencies do not differ much for the steel/PMMA medium with a thickness h of 1·034 mm and various layer thick ratios (h_1/h). In Figure 6, "short time" denotes the result without involving the long-wave assumption (small ω) and "long wave" denotes the result with the long-wave assumption. The result indicates that the expression given by equation (33) is valid not only for very low frequencies but also for relatively large frequencies (1 MHz). The

valid range of frequency is related to the magnitude of t_0. A small t_0 allows equation (33) to be valid for high frequencies, while a large t_0 makes equation (33) valid for low frequencies. Usually, t_0 is very small for a layered medium with thin layers.

The second extreme case is short waves with very large values of ω. Letting $\omega \to \infty$, we obtain from equations (26) to (29)

$$\omega C_1 \approx 1 - e^{-t_0/\tau}\cos \omega t_0, \qquad \omega^2 C_2 \approx \omega e^{-t_0/\tau}\sin \omega t_0 + \frac{1}{\tau}(1 - e^{-t_0/\tau}\cos \omega t_0), \tag{34}$$

$$\omega C_3 \approx -t_0 e^{-t_0/\tau}\cos \omega t_0, \qquad \omega^2 C_4 \approx \omega t_0 e^{-t_0/\tau}\sin \omega t + \xi G_\infty \cos \omega t_0 - 1.$$

Subsequently, from equations (24), (25) and (34), we find

$$G_1(\omega) \approx \xi, \qquad \omega G_2(\omega) \approx \frac{2\xi}{\tau} - \frac{1}{\tau}(\xi e^{-t_0/\tau} + G_\infty)\cos \omega t_0. \tag{35, 36}$$

By using equations (35) and (36), we obtain, from equation (13), the attenuation factor for short waves ($\omega \to \infty$) as

$$\eta = \rho^{1/2}\left[2 - \left(e^{-t_0/\tau} + \frac{1}{\xi}G_\alpha\right)\cos \omega t_0\right] \Big/ (2\tau\xi^{1/2}). \tag{37}$$

Equation (37) gives an oscillatory attenuation factor with the frequency. The mean of the attenuation factor given by equation (40) for short waves, η_{mean}, is

$$\eta_{mean} \approx \frac{\rho^{1/2}}{\tau\xi^{1/2}}. \tag{38}$$

Using (21), the mean of the attenuation factor from (38) becomes

$$\eta_{mean} = \frac{\ln \theta}{h}. \tag{39}$$

The above expression is identical to the wave front decay factor γ given by equation (11). Thus, the attenuation for short waves propagating in a layered medium is equivalent to its wave front decay. This conclusion was stated in reference [4] without a proof.

3.2. EFFECT OF THICKNESS AND IMPEDANCE RATIOS

The short-time relaxation function (20) was used to study the relation between the spatial attenuation factor and the typical cell thickness ratio as well as material properties. The constituent layer thickness ratio (h_1/h or h_2/h) is a measurement of the volume fraction of the constituent materials. For illustration purposes, two sets of material systems, ceramic/aluminum and ceramic/rubber, were studied. The two material systems represented a low impedance mismatch and a high impedance mismatch respectively. Their mechanical properties are given in Table 1.

Figures 7 and 8 show the effects of the thickness ratio and the material impedance mismatch on attenuation. The curves shown in Figures 7 and 8 represent ceramic/rubber with an impedance ratio of 460 and ceramic/aluminum with an impedance ratio of 2.5 respectively. Since the formulation derived for long waves is valid for quite a large range of frequency given that the typical thickness h is small, we therefore, choose the frequency ω as 1 Hz for computational convenience.

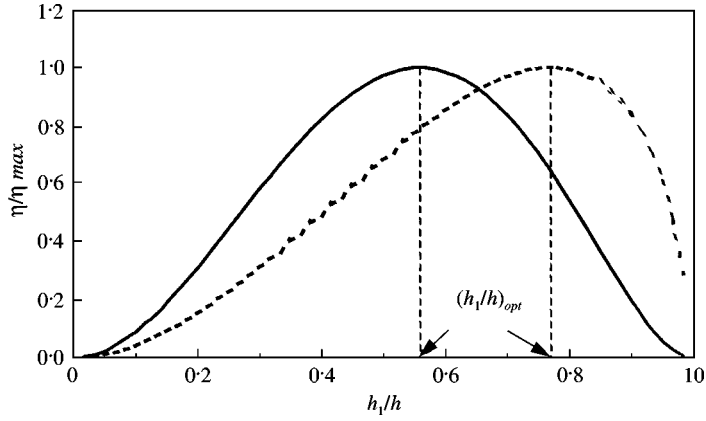

Figure 7. Effect of thickness ratios on the attenuation factor (- - - -, impedance ratio = 460; ——, impedance ratio = 2·5).

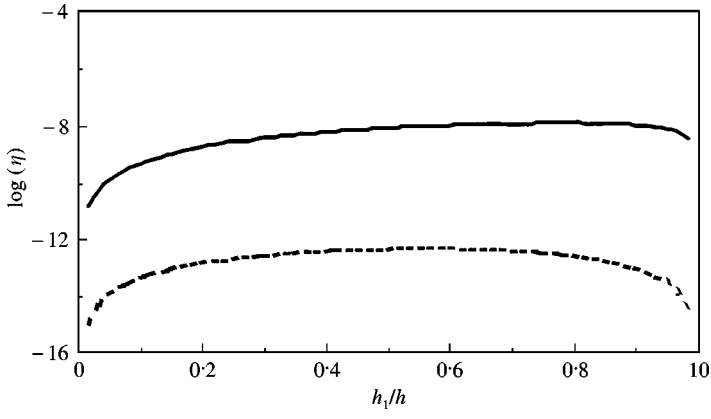

Figure 8. Effect of impedance mismatches on the attenuation factor (——, impedance ratio = 460; - - - -, impedance ratio = 2·5).

It is clearly shown in Figure 7 that there is a thickness ratio that gives the maximum attenuation factor. The thickness ratio of maximum attenuation, $(h_1/h)_{opt}$, depends on the impedance mismatch of the two constituent materials. Given a typical thickness h, $(h_1/h)_{opt}$ is around 0·55 for ceramic/aluminum, while $(h_1/h)_{opt}$ is about 0·78 for ceramic/rubber. In other words, the layer with high impedance needs to be thicker in order to achieve the maximum attenuation if the impedance mismatch of the two constituent materials is high. It is also shown in Figure 7 that the attenuation factor vanishes as the thickness ratio (h_1/h) approaches the two extreme cases, i.e., $h_1/h = 0$ (a homogeneous medium of material 2) and $h_1/h = 1$ (a homogeneous medium of material 1). A thickness ratio $h_1/h = 0{\cdot}5$ gives an attenuation factor close to the maximum.

Figure 8 shows the effect of impedance mismatch. It is seen that the attenuation increases as impedance mismatch increases.

Note that the attenuation factor is frequency dependent. Nonetheless, additional numerical results indicate that Figures 7 and 8 hold for a wide range of frequency up to the order of 1 MHz for the given geometry and material systems.

In the rest of this section, we verified the maximum attenuation achieved in the previous discussion by illustrations of stress wave propagation in a layered ceramic/aluminum medium as an example.

Wave propagation was solved by using equation (6) for stress responses at the mid-planes in the odd-numbered layers and its extensions for arbitrary positions based upon the exact relaxation function (1) (see reference [2]). The method of inverse Laplace transformation discussed in reference [12] was used in this computation. Layered media constituted by the same materials with the same typical cell thickness $h = 3{\cdot}0$ mm but different layer thickness ratios (defined as h_1/h) were examined. A unit step stress was applied at the mid-plane of the first layer (layer 1) of the layered medium at time $t = 0$. For demonstration purposes, three representative thickness ratios were chosen, i.e., $(h_1/h)_{opt} = 0{\cdot}55$ which corresponds to the maximum attenuation, $h_1/h = 0{\cdot}2$ which is less than $(h_1/h)_{opt}$, and $h_1/h = 0{\cdot}8$ which is larger than $(h_1/h)_{opt}$. In order to compare the attenuation effect of waves in the layered media properly, a comparison is made at the same spatial positions but equivalent time (when the wave front propagates the same distance in different media).

Figure 9 shows the wave fronts and their trailing profiles of the stress responses in a layered medium at three different times ($t = t_0$, $t = t_0 + \Delta t$, and $t = t_0 + 2\Delta t$, where Δt is the time needed for a wave front to pass through a typical cell, calculated differently for each medium) when the wave front reaches $x/h = 13$, 14, and 15 respectively. To make the comparison clearer, we incorporated the wave responses of the other two media into the medium with a thickness ratio equal to $(h_1/h)_{opt}$, respectively [see Figure 9(a,b)]. The marked points in Figure 9 represent the computed exact values of the stress wave at the corresponding positions in time. The linking lines between markers are drawn for an outlining purpose.

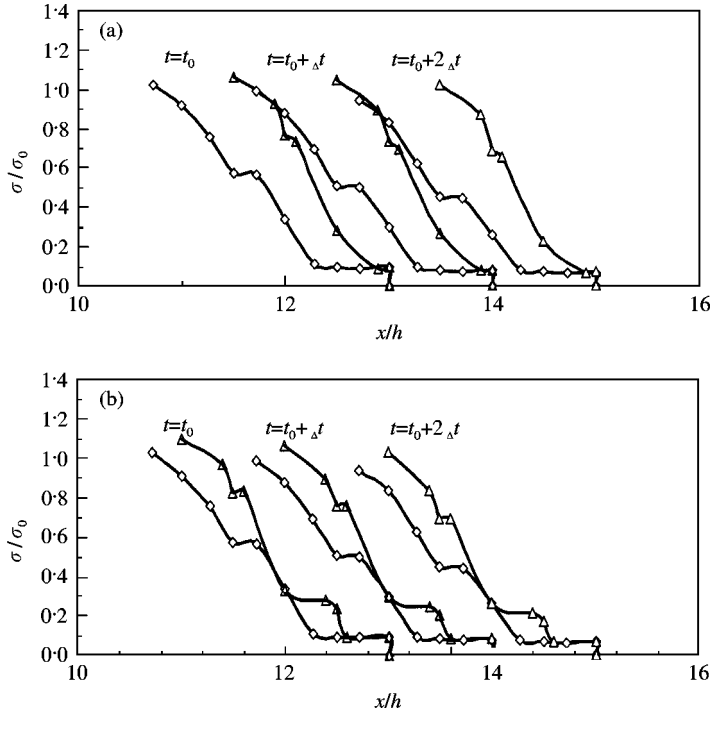

Figure 9. Wave fronts and their trailing profiles in layered media with different thickness ratios. (a) —◇—, $h_1/h = (h_1/h)_{opt}$; and —△—, $h_1/h < (h_1/h)_{opt}$; (b) —◇—, $h_1/h = (h_1/h)_{opt}$; and —△—, $h_1/h > (h_1/h)_{opt}$.

Since the number of interfaces of all the three-layered media with different thickness ratios is identical in the comparison, the wave front decays in all the cases should be identical as discussed in section 2.2. Figure 9 confirms this point. The wave fronts in all the three layered media are identical. However, the trailing waves do differ. The medium with a layer thickness ratio equal to $(h_1/h)_{opt}$ always results in a flatter wave profile trailing the wave front, indicating a greater spatial attenuation effect. This can be understood in this way. Consider the two media subjected to the same unit step loading. After the stress wave propagating the same distance, one of its wave profiles becomes flatter than the other. The one that has flatter wave profiles must have experienced a higher attenuation in the course of propagation through the given distance, or a higher spatial attenuation. In addition, by checking the attenuation rate of the two corresponding positions (excluding the wave front and its immediate neighborhood) from one typical cell to the next adjacent typical cell (with time difference Δt), we found that the medium with the optimal cell thickness ratio $(h_1/h)_{opt}$ has the highest attenuation rate. Thus, the medium with $(h_1/h)_{opt}$ demonstrates the highest spatial attenuation effect among the three media.

The following could be summarized in accordance with Figure 9.

- Different thickness ratios result in different spatial attenuations for stress waves propagating in layered media with the same constituent materials and the same cell thickness, h.
- The highest attenuation occurs in the layered medium with the thickness ratio $(h_1/h)_{opt}$, which agrees very well with the results calculated by the attenuation factor derived from equation (33).

It is worth pointing out that the propagation and attenuation of waves in a layered elastic medium is different from the propagation and attenuation of waves in a homogeneous viscoelastic medium. The wave produced by a unit step stress in a layered elastic medium can have an amplitude exceeding the input unit amplitude (which an the wave responses beyond the trailing portion of a wave front, not shown in Figure 9), while the amplitude of the wave produced by the same input in conventional homogeneous viscoelastic media can never exceed the input magnitude [8, 13]. This is why the attenuation calculation is only valid for a short time after the passage of the wave front.

3.3. EFFECT OF CELL THICKNESS

We considered the material system of ceramic/aluminum with the properties listed in Table 1 and calculated the attenuation factor given by equation (33) to make a comparison among three media with cell thickness equal to $h_0/2$, h_0, and $2h_0$, respectively, where h_0 is an arbitrary thickness. For a given distance, a layered medium with thinner cells contains more layers than a layered medium with thicker cells. For a frequency of 1 Hz (wavelength $\approx$ 8000 m) and $h_0 = 3$ mm, the calculated results are presented in Figure 10. It is evident that the layered medium with thicker cells gives a larger spatial attenuation factor than that with thinner cells. On the other hand, the wave front decay shows an opposite trend. This behavior is easy to understand by noting that the wave front decay factor γ only depends on the number of interfaces it passes.

The above discussion was checked against the study of wave propagation in the ceramic/aluminum layered medium. Two cell thicknesses were considered, i.e., $h = h_0$, and $2h_0$, with $h_0 = 3$ mm. The thickness ratio h_1/h was assumed to be 0·2 for both layered media. We propagated a unit step stress wave at $x = 0$ into the layered media and checked the stress response at a certain position.

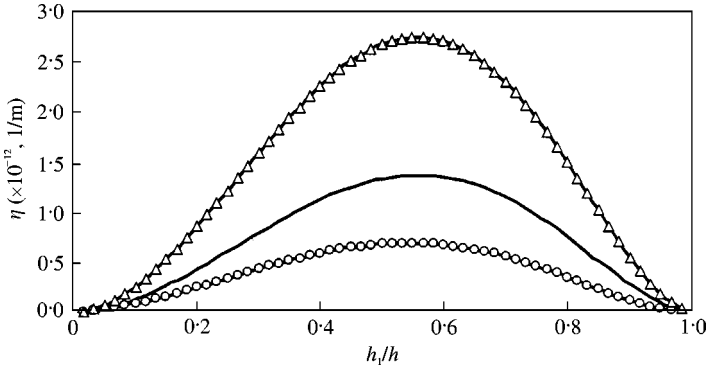

Figure 10. Effect of the cell thickness on the attenuation factor (—○—, $h = h_0/2$; —, $h = h_0$; —△—, $h = 2h_0$).

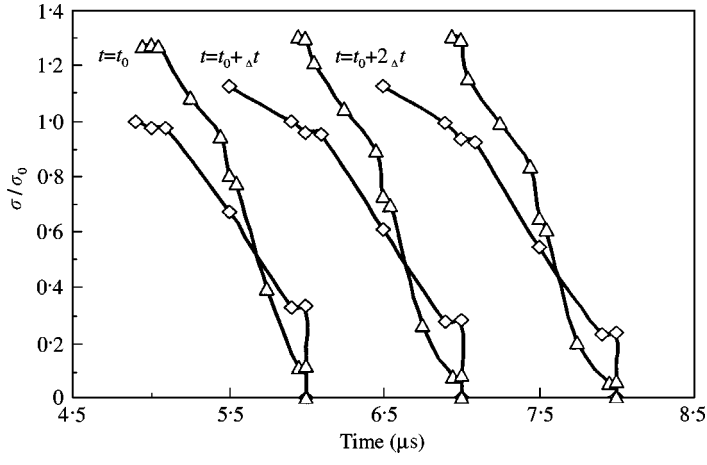

Figure 11. Wave fronts and their trailing of a step stress wave propagating in two layered media with different cell thicknesses (—△—, $h = h_0$; —◇—, $h = 2h_0$).

Figure 11 shows the stress responses of the wave in the two media. The curves in Figure 11 are the wave front as well as its trailing stage at three different times which correspond to the wave front reaching $x = 12h_0$, $14h_0$, and $16h_0$ respectively. The results indicate that the medium of thinner cells ($h = h_0$) provides a greater decay than the medium of thicker cells ($h = 2h_0$) at the wave front. On the other hand, the slope of the trailing wave profile behind the wave front in the medium with thicker cells is flatter. This agrees with the results depict in Figure 10 which shows that a layered medium of thicker cells has a higher spatial attenuation than a layered medium of thinner cells.

Based upon the above discussions, we note that there are two different features in the effect of cell thickness, i.e., wave front decay and spatial attenuation. For a layered medium with thinner cells, the decay of a stress wave at the wave front is greater but its rise to a certain amplitude is spatially shorter. The opposite is true for a layered medium with thicker cells. An optimal design for a layered medium in the layer thickness depends on the selection of wave front decay or the spatial attenuation as the objective function.

4. CONCLUSION

The wave front decay and the spatial attenuation of the trailing wave in an elastic media consisting of alternating layers of different materials have been studied. With the short-time relaxation function model, it was shown that the short-wave attenuation characterizes the wave front decay, while the long-wave attenuation is related to the spatial attenuation. The proposed short-time relaxation function agrees very well with the exact one in describing the wave front decay and the spatial attenuation for waves trailing the wave front. The following conclusions have been reached.

(1) An analogy in the attenuation behavior between layered elastic media and homogeneous viscoelastic media exists at the wave front and its immediate trailing wave.
(2) Given that other conditions are the same, the thickness ratio of the two constituent layers can affect the attenuation of waves trailing the wave front in the periodically layered elastic medium. In general, the attenuation effect decreases as the ratio of the two constituent layer thicknesses (h_1/h for example) approaches either 0 (homogeneous medium of material 1) or 1 (homogeneous medium of material 2).
(3) The cell thickness affects the decay of the wave front and the spatial attenuation. A thinner cell results in a greater decay of the wave front but in a smaller spatial attenuation of waves trailing the wave front.
(4) A higher impedance mismatch between the two constituent materials leads to a higher spatial attenuation of waves trailing the wave front and to a larger wave front decay for the material systems studied.

ACKNOWLEDGMENT

This work was supported by an Army Research Office MURI Grant no. DAAH04-96-1-0331 to Purdue University.

REFERENCES

1. L. M. Barker 1971 *Journal of Composite Materials* **5**, 140–162. A model for stress wave propagation in composite materials.
2. T. C. T. Ting and I. Mukunoki 1979 *Journal of Applied Mechanics* **46**, 329–336. A theory of viscoelastic analogy for wave propagation normal to the layering of a layered medium.
3. I. Mukunoki and T. C. T. Ting 1980 *International Journal of Solids and Structures* **16**, 239–251. Transient wave propagation normal to the layering of a finite layered medium.
4. R. M. Christensen 1973 *Journal of Applied Mechanics* **40**, 155–160. Attenuation of harmonic waves in layered media.
5. R. M. Christensen 1975 *Journal of Applied Mechanics* **42**, 153–158. Wave propagation in layered elastic media.
6. F. C. Karal, Jr. and J. B. Keller 1964 *Journal of Mathematical Physics* **5**, 537–547. Elastic, electromagnetic and other waves in a random medium.
7. L. M. Brekhovskikh 1973 *Waves in Layered Media*. New York: Academic Press, second edition, 1980.
8. W. Flugge 1967 *Viscoelasticity*. Waltham, MA: Blaisdell Publishing Company.
9. R. M. Christensen 1971 *Theory of Viscoelasticity*: *An Introduction*. New York: Academic Press.
10. A. S. Nowick and B. S. Berry 1972 *Anelastic Relaxation in Crystalline Solids*. New York: Academic Press.
11. R. E. Bellman, R. Kalaba and J. A. Lockett 1966 *Numerical Inversion of the Laplace Transform*: *Applications to Biology*, *Economics Engineering and Physics*. New York: American Elsevier Publishing Company, Inc.
12. F. Durbin 1974 *The Computer Journal* **17**, 371–376. Numerical inversion of Laplace transforms: an efficient improvement to Dubner and Abate's method.
13. C. T. Sun 1970 *Journal of Applied Mechanics* **37**, 1171–1144. Transient wave propagation in viscoelastic rods.